Vol 16 No 2, February 2007
1009-1963/2007/16(02)/0499-07

Chinese Physics

© 2007 Chin. Phys. Soc.
and IOP Publishing Ltd

Thermoelasticity of CaO from first principles*

Liu Zi-Jiang(刘子江)[a)b)c)], Qi Jian-Hong(祁建宏)[a)], Guo Yuan(郭 媛)[a)],
Chen Qi-Feng(陈其峰)[b)†], Cai Ling-Cang(蔡灵仓)[b)], and Yang Xiang-Dong(杨向东)[c)]

[a)] *Institute of Electronic Information Science and Technology, Lanzhou City University, Lanzhou* 730070, *China*
[b)] *Laboratory for Shock Wave and Detonation Physics Research, Institute of Fluid Physics, P. O. Box* 919-102, *China Academy of Engineering Physics, Mianyang* 621900, *China*
[c)] *Institute of Atomic and Molecular Physics, Sichuan University, Chengdu* 610065, *China*

(Received 2 June 2006; revised manuscript received 18 August 2006)

The thermoelastic properties of CaO over a wide range of pressure and temperature are studied using density functional theory in the generalized gradient approximation. The transition pressure taken from the enthalpy calculations is 66.7 GPa for CaO, which accords with the experimental result very well. The athermal elastic moduli of the two phases of CaO are calculated as a function of pressure up to 200 GPa. The calculated results are in excellent agreement with existing experimental data at ambient pressure and compared favourably with other pseudopotential predictions over the pressure regime studied. It is also found that the degree of the anisotropy rapidly decreases with pressure increasing in the B1 phase, whereas it strongly increases as the pressure increases in the B2 phase. The thermodynamic properties of the B1 phase of CaO are predicted using the quasi-harmonic Debye model; the heat capacity and entropy are consistent with other previous results at zero pressure.

Keywords: thermoelasticity, high pressure, first principles, quasi-harmonic Debye model
PACC: 6740K, 6220D, 6400

1. Introduction

CaO is a major constituent in the lower mantle,[1] and its thermoelasticity is important for our understanding the processes including brittle failure, flexure, and the propagation of elastic waves.[2,3] However, many of its physical properties are still relatively poorly understood. For example, its equation of state (EOS) is relatively well known only at 298 K,[4−6] while at high pressures and temperatures no experiments are reported. The elastic constants are studied experimentally at pressures only up to 1 GPa,[7] although elasticity data are available over a wide temperature range.[8] Chang and Graham [7] have investigated several thermodynamical quantities of CaO at zero pressure and 298 K only. Moreover, there have existed no measurements about thermodynamic properties of CaO at high pressures. The pressure-induced transition from the B1 phase to the B2 phase was observed in both diamond cell and shock wave experiments at pressures ranging from 53 to 70 GPa.[4−6,9] A number of theoretical investigations of structure and phase stability of CaO at high pressures have been made, indicating that the B1–B2 phase transition takes place in a wide range of predicted pressures.[10−18] Correspondingly, first-principles computer simulations have been increasingly employed for exploring various properties of the Earth's materials under the geophysically relevant conditions. The full-potential linear muffin-tin-orbital (FP–LMTO) was used to study the elastic properties and their pressure dependence of four B1-type alkaline earth oxides at high pressures.[19] Recently, Karki and Crain [12] have performed plane-wave pseudopotential (PWPP) calculations to predict single crystal elastic constants of CaO as a function of pressure up to 140 GPa.

In this paper, we present first-principles predictions of elasticity of CaO at high pressures using the plane-wave pseudopotential in the generalized gradient approximation. Our results are comparable with the previous ones at high pressures.[19] The thermo-

*Project supported by the National Natural Science Foundation of China (Grant Nos 10574096 and 10674120), the Specialized Research Fund for the Doctoral Program of Higher Education of China (Grant No 20050610010), the Natural Science Foundation of Gansu Province, China (Grant No 3ZS051-A25-027) and the Scientific Research Foundation of Education Bureau of Gansu Province, China (Grant No 0410-01).
†Corresponding author. E-mail: lzjcaep@126.com.

dynamic properties of the B1 phase of CaO at high pressures and temperatures are predicted using the quasi-harmonic Debye model.

2. Method

All the calculations are performed using the CASTEP (Cambridge Serial Total Energy Package) code.[20] The CASTEP is a state of the art quantum mechanics based program designed specifically for solid state materials science. The CASTEP employs the density functional theory (DFT)[21] plane-wave pseudopotential method that allows performing first-principles quantum mechanics calculations to explore the properties of crystals and surfaces in materials such as semiconductors, ceramics, metals, minerals, and zeolites. In this paper, the exchange-correlation functional theory is adopted in the generalized gradient approximation (GGA),[22] which is the most advanced approximation currently available in DFT. In addition, the ultrasoft pseudopotentials[23] are employed for Ca and O. All the pseudopotentials are non-local. The core radii are 1.06 Å for Ca, and 0.74 Å for O. The use of an ultrasoft pseudopotential allows us to use a relatively small basis set with a plane wave cut-off energy of 380 eV without any loss of accuracy and with excellent convergence of all properties with respect to the basis set (the maximum stress is only 0.02 GPa). The Brillouin zone is sampled on a $9 \times 9 \times 9$ Monkhorst–Pack k-point mesh,[24] which provides convergence of the total energy to a value within 5.0×10^{-6} eV/atom. The Kohn–Sham equations are solved iteratively to self-consistency within 5.0×10^{-7} eV/atom.

The determination of the elastic constants requires the knowledge of equilibrium structure at a given pressure. We first fully optimize a single primitive cell of CaO at several pressures. The structural optimization problem can be effectively solved by employing the Broyden–Fletcher–Goldfarb–Shanno technique[25] with a variable cell shape.[26] The elastic constants are then determined from direct computation of the stresses generated by small deformations of the equilibrium unit cell. Strains of different amplitudes (-0.003 to 0.003) are used and the elastic constants are derived from the resulting nonlinear stress–strain relation.[27] The details of the computational method have been given elsewhere.[28]

To investigate the thermodynamic properties of CaO, we here apply the quasi-harmonic Debye model,[29] in which the non-equilibrium Gibbs function $G^*(V;p,T)$ takes the following form:[29]

$$G^*(V;p,T) = E(V) + pV + A_{\rm vib}(\Theta(V);T), \quad (1)$$

where $\Theta(V)$ is the Debye temperature, and the vibrational term $A_{\rm vib}$ can be written as[30,31]

$$A_{\rm vib}(\Theta;T) = nkT\left[\frac{9}{8}\frac{\Theta}{T} + 3\ln(1-{\rm e}^{-\Theta/T}) - D\left(\frac{\Theta}{T}\right)\right], \quad (2)$$

where $D(\Theta/T)$ represents the Debye integral, n is the number of atoms per formula unit. For an isotropic solid, Θ is expressed as[30]

$$\Theta = \frac{\hbar}{k}\left[6\pi^2 V^{1/2} n\right]^{1/3} f(\sigma)\sqrt{\frac{B_s}{M}}, \quad (3)$$

where M is the molecular mass per formula unit, B_s the adiabatic bulk modulus, which can be approximated by the static compressibility[29]

$$B_s \simeq B(V) = V\left(\frac{{\rm d}^2 E(V)}{{\rm d}V^2}\right). \quad (4)$$

Here the Poisson ratio σ is taken as 0.25,[32] $f(\sigma)$ is given in Refs.[33,34]. Therefore, the non-equilibrium Gibbs function $G^*(V;p,T)$ as a function of $(V;p,T)$ can be minimized with respect to volume V as follows:

$$\left(\frac{\partial G^*(V;p,T)}{\partial V}\right)_{P,T} = 0. \quad (5)$$

By solving Eq.(5) we obtain the thermal EOS. The isothermal bulk modulus B_T, the heat capacity C_V, the entropy S and the thermal expansion coefficient α are given respectively by[34]

$$B_T(p,T) = V\left(\frac{\partial^2 G^*(V;p,T)}{\partial V^2}\right)_{P,T}, \quad (6)$$

$$C_V = 3nk\left[4D\left(\frac{\Theta}{T}\right) - \frac{3\Theta/T}{e^{\Theta/T}-1}\right], \quad (7)$$

$$S = nk\left[4D\left(\frac{\Theta}{T}\right) - 3\ln\left(1-e^{-\Theta/T}\right)\right], \quad (8)$$

$$\alpha = \frac{\gamma C_V}{B_T V}, \tag{9}$$

where γ is the Grüneisen parameter.

3. Results and discussion

3.1. Static equation of state

For the B1 phase of Cao, the lattice constant, bulk modulus, and its pressure derivative are obtained by calculating the total energy and pressure for different values of the unit cell volume and by fitting the calculated data to the third-order Birch–Murnaghan EOS as shown below:[35]

$$P(x) = \frac{3}{2}K_0\left[x^{7/3} - x^{5/3}\right]\left\{1 + \xi\left[x^{2/3} - 1\right]\right\}, \tag{10}$$

$$E(x) = E_0 + \frac{3}{2}K_0V_0\left[\frac{3}{2}(\xi - 1)x^{2/3} + \frac{3}{4}(1 - 2\xi)x^{4/3} + \frac{1}{2}\xi x^{6/3} - \frac{2\xi - 3}{4}\right], \tag{11}$$

where $x = V_0/V$ and $\xi = \frac{3}{4}(K_0' - 4)$. V_0 is the unit-cell volume at zero pressure, K_0 is the bulk modulus, and K_0' is the pressure derivative of the bulk modulus at zero pressure. Errors from the numerical fitting are less than 2 GPa for the experimental bulk modulus and less than 0.02 for K_0'.[6] The calculated equilibrium lattice constants, bulk modulus, and their pressure derivatives are given in Table 1.

Table 1. Lattice constant, unit cell volume, bulk modulus and pressure derivatives for the B1 phase of CaO from the calculations and measurements.

Method	a_0/Å	V_0/Å^3	K_0/GPa	K_0'
PWPP GGA (this work)	4.816	111.7	109.3	4.28
FP–LAPW LDA[36]	4.72	105.15	128.0	4.11
LCAO–SCF[37]	4.71–4.86	104.5–114.8	117–134	-
AIM[11]	4.809	111.2	116.1	-
FP–LMTO GGA[19]	4.840	113.4	109.0	4.00
PWPP LDA[12]	4.838	113.2	117	4.41
PIB[16]	4.82	111.98	102	4.33
Experiment[6]	4.811	111.35	110.0	4.26

Our results are comparable with the previous ones.[11,12,16,19,36,37] The pressure dependence of the volume for CaO calculated with the PW91[22] functional is shown in Fig.1. It is found that the calculated EOS of CaO is in excellent agreement with the experimental data.[4–6]

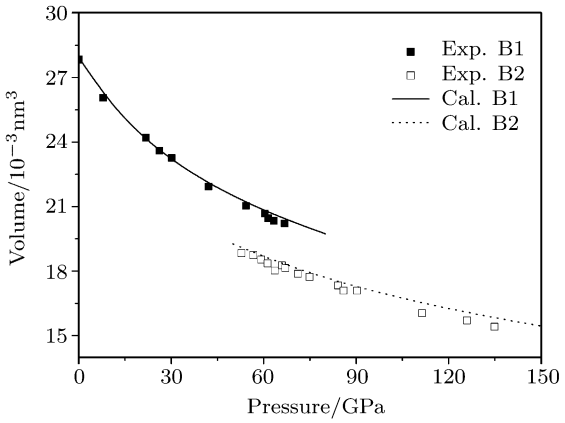


Fig.1. Static equation of state of CaO. Theoretical data of the B1 and B2 phases are represented by solid and dotted lines, respectively. Experimental data of the B1 and B2 phases at room temperature are denoted by solid and open squares, respectively (Ref.[4–6]).

3.2. B1–B2 phase transition

We calculate the enthalpy of the two-ion primitive cell of CaO in both the B1 (NaCl) and B2 (CsCl) structures as a function of pressure from 0 to 150 GPa (Fig.2). The thermodynamic requirement for the equality of free energies at a phase boundary suggests that the B1–B2 transition pressure of CaO should occur at 66.7 GPa. The transition involves the volume decreasing by 10.4%, suggesting clearly its first-order character. The B1–B2 transition involves the coordination number increasing from 6 for the NaCl structure to 8 for the CsCl structure, resulting in denser packing. As the coordination increases, the first nearest-neighbour (Ca–O) distances increase but the second nearest-neighbour distances decrease, resulting in a finite volume collapse at the transition. We have compared the predicted B1–B2 transition in CaO with the previous measurements[4–6,9] and calculations[10–18] in Table 2. Although our predicted value is much larger than some previous calculations, it falls to in an experimental range of 53–

70 GPa,[4−6,9] and agrees well with the latest theoretical result.[10] The differences among all theoretical data result from the different methods used.[38] Moreover, it is also pointed out[39,40] that usually the local density approximation (LDA) underestimates transition pressures, whereas the GGA overestimates them slightly (by a few GPa). The linearized augmented plane wave (LAPW) method has been used to predict the transition pressure of 54 GPa and a volume collapse of about 12% at the transition.[15] The calculations based on potential-induced breathing (PIB)[16] and modified PIB[14] models have shown that the transition should occur at 55 and 61 GPa, respectively, whereas the modified electron gas (MEG)[18] and augmented plane wave (APW)[17] methods have given quite different transition pressures of 121 and 32 GPa, respectively.

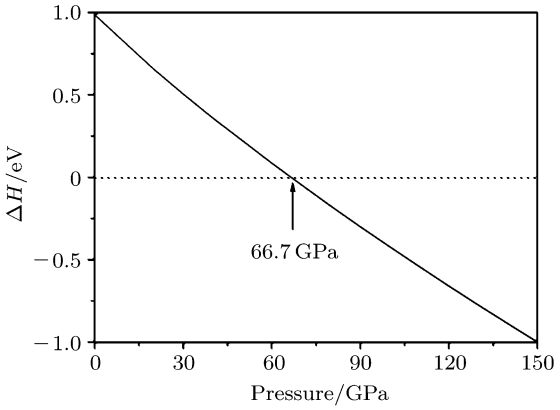


Fig.2. The enthalpy difference between the B1 phase and B2 phase as a function of pressure.

Table 2. The B1–B2 phase transition pressure of CaO.

Method	P_{tr}/GPa
PWPP GGA (this work)	66.7
LCAO GGA[10]	64.7
AIM[11]	63.0
PWPP LDA[12]	57.6
TBLMTO[13]	55.7
MPIB[14]	61
LAPW[15]	54.2
PIB[16]	55.0
APW[17]	32
MEG[18]	121
Experiment[4−6,9]	53–70

3.3. Elastic moduli

The calculated athermal elastic constants at zero pressure are found to compare favourably with the measurements[7,8] in Table 3. The small differences from the measurements can be attributed to the fact that the calculations are athermal whereas experimental data are obtained at 300 K. Most of the differences between the present elastic constants and the other pseudopotential results[11,12,16,18,19] can be accounted for. Overall, first-principles theory represents a substantial improvement on the predictions of more approximate theories, such as those based on simplified semiempirical[16] and ab initio models.[18]

Table 3. Three elastic constants (c_{ij}), and bulk (K) and shear (G) moduli in GPa of CaO (B1 structure) compared with previous results at zero pressure.

Method	c_{11}	c_{12}	c_{44}	K	G
PWPP GGA (this study)	207	58	76	107	77
FP-LMTO GGA[19]	223	53	84	110	85
PWPP LDA[12]	241	52	77	115	83
AIM[11]	232	58	73	116	-
PIB[16]	206	50	66	102	71
MEG[18]	207	97	97	134	77
Experiment[7,8]	222	58	80	113	84

The effect of pressure on the elastic constants of CaO is large, so experimental or theoretical results at ambient pressure cannot be used to reliably estimate elasticity at mantle pressures. Therefore, we predict the elastic constants of CaO. The bulk modulus of isotropic aggregate of cubic crystals is related to the elastic constant $K = (c_{11} + 2c_{12})/3$. The pressure dependence of the isotropic aggregate shear modulus (G) of CaO is obtained using the Hashin *et al*[41] averaging scheme. In Fig.3 and Fig.4, the elastic moduli of the two phases of CaO are shown as a function of pressure and compared with the linear extrapolation

of the experimental data[7] from low pressure to high pressure.

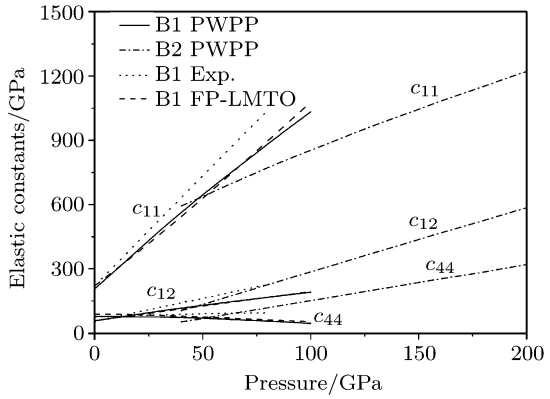


Fig.3. Pressure dependence of elastic constants of CaO. Solid and dash dotted lines represent elastic constants of the B1 and B2 phases, respectively. FP–LMTO results of the B1 phase are denoted by dashed line (Ref.[19]). Experimental data of the B1 phase are shown by dotted lines (Ref.[7]).

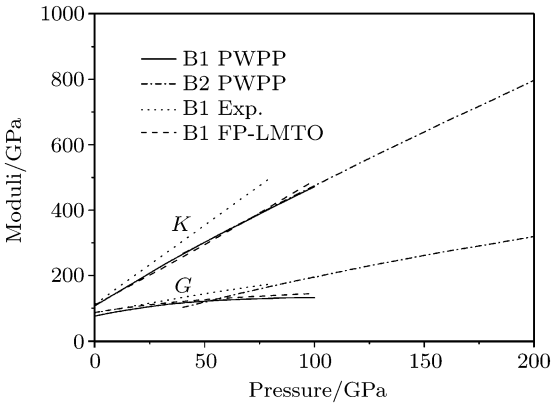


Fig.4. Pressure dependence of bulk and shear moduli of CaO. Solid and dash dotted lines represent elastic constants of the B1 and B2 phases, respectively. FP–LMTO results of the B1 phase are denoted by dashed line (Ref.[19]). Experimental data of the B1 phase are shown by dotted lines (Ref.[7]).

The calculated values of all elastic moduli of the B1 phase of CaO are slightly underestimated in comparison with the experimental values, which, however, are in good agreement with the latest theoretical data[19] over a wide pressure range. We also find that with increasing pressure both c_{11} and c_{12} increase, but c_{44} weakens beyond 10 GPa in the B1 phase. On the other hand, c_{11} increases weakly, and c_{12} increases strongly with the increase of pressure in the B2 phase compared with those of B1 phase, and c_{44} and G strengthen strongly with pressure increasing.

CaO is cubic and its second-rank tensor properties (e.g. thermal expansion, dielectric constants, and compressibility) are isotropic. However, elasticity, which is a fourth-rank tensor property, is anisotropic even for cubic crystals, where it is conveniently expressed by the dimensionless parameter anisotropy factor $A = (2c_{44} + c_{12})/c_{11} - 1$. The pressure dependence of the anisotropy factor A is shown in Fig.5. The anisotropy factor A drops off rapidly with the increase of pressure initially, and then decreases more slowly at higher pressures in the B1 phase, whereas it increases strongly with the increase of pressure in the B2 phase, showing a finite jump in the degree of the anisotropy at the transition pressure. Different pressure variations of the anisotropy factor A in the B1 and B2 phases result from the weakening of c_{44} (in the B1 phase), and ultimately lead to a shear instability of the B1 structure at a much higher pressure. The theoretically predicted behaviour of CaO is consistent with the experimental one[7] at zero pressure and other ones in Ref.[19].

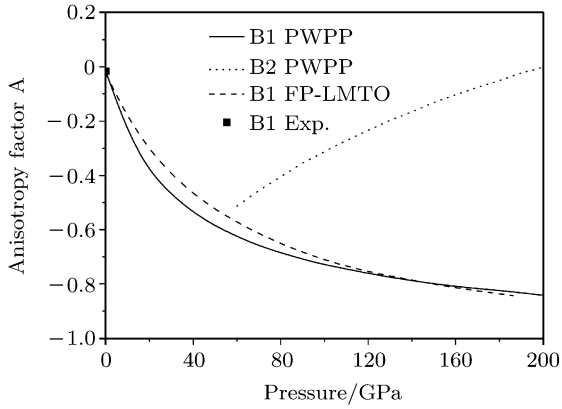


Fig.5. Pressure dependence of anisotropy factor A of CaO. Solid and dotted lines represent anisotropic factors of the B1 and B2 phases, respectively. FP–LMTO results of the B1 phase are denoted by dashed line (Ref.[19]). Experimental data of the B1 phase are shown by solid square (Ref.[7]).

3.4. Thermodynamic properties

Figure 6 shows the calculated and measured thermal expansions (α) of the B1 phase of CaO. One can see that the neglect of intrinsic anharmonicity in the quasi-harmonic approximation leads to an overestimation of thermal expansion, which is rather spectacular at zero pressure and 300 K. α is found to increase rapidly at lower temperatures, and rapidly flattens out with increasing temperature. As pressure increases, α

decreases rapidly and the effects of temperature become less and less pronounced, resulting in linear high temperature behaviour. It is shown that α converges to a constant value at high temperatures and high pressures.

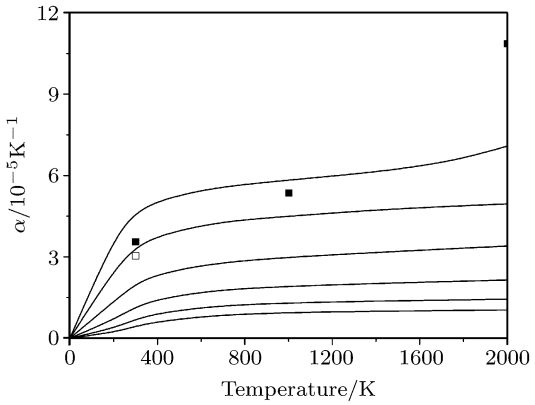


Fig.6. Pressure and temperature dependences of thermal expansivity of the B1 phase of CaO. The isobars at 0, 10, 30, 60, 100, and 150 GPa are represented by solid lines from top to bottom. Experimental value at zero pressure and 300 K is denoted by an open square (Ref.[7]). Solid squares are for the calculated data by Karki and Wentzcovitch at zero pressure and 300, 1000, and 2000 K, respectively (Ref.[42]).

The heat capacity at a constant pressure (C_P) is given by $C_P = C_V(1 + \alpha\gamma T)$. The predicted values of C_V, C_P and S of the B1 phase of CaO in ambient condition are 41.72, 42.91, and 38.12 $Jmol^{-1}K^{-1}$, respectively. Theoretical values of the C_V and S are compared respectively in Fig.7 and Fig.8.

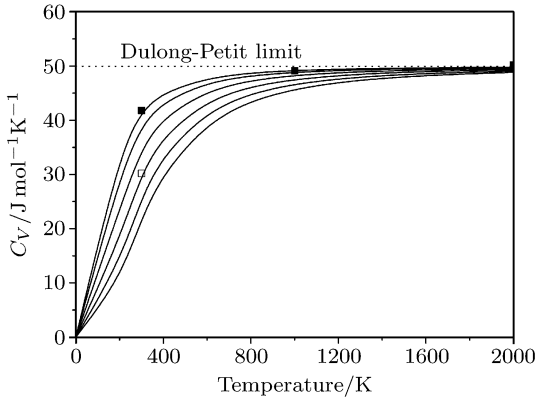


Fig.7. Pressure and temperature dependences of heat capacity of the B1 phase of CaO. The isobars at 0, 10, 30, 60, 100, and 150 GPa are represented by solid lines from top to bottom. Experimental data at zero pressure and 300 K is denoted by an open square (Ref.[7]). Solid squares are for the calculated data by Karki and Wentzcovitch at zero pressure and 300, 1000, and 2000 K, respectively (Ref.[42]).

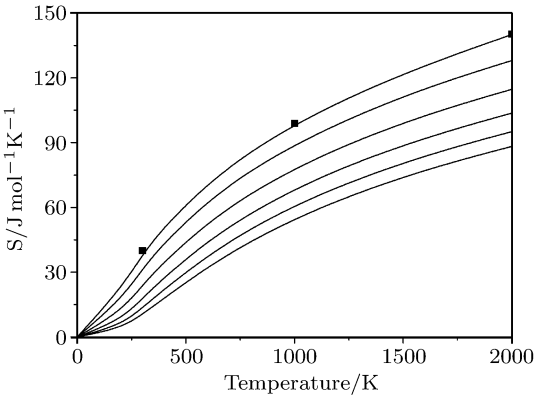


Fig.8. Pressure and temperature dependences of entropy of the B1 phase of CaO. The isobars at 0, 10, 30, 60, 100, and 150 GPa are represented by solid lines from top to bottom. Solid squares are for the calculated data by Karki and Wentzcovitch at zero pressure and 300, 1000, and 2000 K, respectively (Ref.[42]).

It is found that the values of C_V and S that we obtained are practically identical with those obtained by Karki and Wentzcovitch [42] but quite different from experimental data[7] at zero pressure and 300 K. Figure 7 illustrates that the anharmonic effects are suppressed at high pressures and C_V is very close to the Dulong–Petit limit at high pressures and temperatures. As shown in Fig.8, unlike α and C_V, the high temperature dependence of S is nearly insensitive to pressure.

4. Conclusions

The first-principles plane wave pseudopotential calculations are performed for the analysis of the structural properties of CaO under high pressure conditions. The calculating results accord with not only the observed pressure-induced volume compressions but also the experimental transition pressures from low-pressure B1 to high-pressure B2 phases. Our calculated elastic moduli of the two phases of CaO at pressures up to 200 GPa are in excellent agreement with the existing experimental data[7] at ambient pressure and the previous calculations at high pressures.[19] It is also found that the degree of the anisotropy rapidly decreases with pressure increasing in the B1 phase, whereas it strongly increases as the pressure increases in the B2 phase. The thermodynamic properties of the B1 phase of CaO are predicted using the quasi-harmonic Debye model. We see that

the predicted heat capacity and entropy are in agreement with the calculated values by Karki and Wentzcovitch [42] at zero pressure. The thermal expansion and heat capacity are shown to converge to a nearly constant value at high pressures and temperatures. Unlike α and C_V, S is nearly insensitive to pressure.

References

[1] Yamanaka T, Kittaka K and Nagai T 2002 *J. Mineral. Petrol. Sci.* **97** 144

[2] Hu J B, Yu Y Y, Dai C D and Tan H 2005 *Acta Phys. Sin.* **54** 5750

[3] Tao Y M, Cao H X and Jiang Q 2005 *Acta Phys. Sin.* **54** 274

[4] Jeanloz R, Ahrens T J, Mao H K and Bell P M 1979 *Science* **206** 829

[5] Mammone J F, Mao H K and Bell P M 1981 *Geophys. Res. Lett.* **8** 140

[6] Richet P, Mao H K and Bell P M 1988 *Geophys. Res. Lett.* **93** 15279

[7] Chang Z P and Graham E K 1977 *J. Phys. Chem. Solids* **38** 1355

[8] Oda H, Anderson O L, Isaak D G and Suzuki I 1992 *Phys. Chem. Miner.* **19** 96

[9] Jeanloz R and Ahrens T J 1980 *Geophys. J. R. Astron. Soc.* **62** 505

[10] Catti M 2003 *Phys. Rev.* B **68** 100101

[11] Aguado A, Bernasconi L and Madden P A 2003 *J. Chem. Phys.* **118** 5704

[12] Karki B B and Crain J 1998 *J. Geophys. Res.* **103** 12405

[13] Kalpana G, Palanivel B and Rajagopalan M 1995 *Phys. Rev.* B **52** 4

[14] Zhang H and Bukowinski M S T 1991 *Phys. Rev.* B **44** 2495

[15] Mehl M J, Cohen R E and Krakauer H 1988 *J. Geophys. Res.* **93** 8009

[16] Mehl M J, Hemley R J and Boyer L L 1986 *Phys. Rev.* B **33** 8685

[17] Bukowinski M S T 1985 *Geophys. Res. Lett.* **12** 536

[18] Cohen A J and Gordon R J 1976 *Phys. Rev.* B **14** 4593

[19] Tsuchiya T and Kawamura K 2001 *J. Chem. Phys.* **114** 10086

[20] Segall M D, Lindan P J D, Probert M J, Pickard C J, Hasnip P J, Clark S J and Payne M C 2002 *J. Phys.: Condens. Matter* **14** 2717

[21] Hohenberg P and Kohn W 1964 *Phys. Rev.* B **136** 864

[22] Wang Y and Perdew J P 1991 *Phys. Rev.* B **44** 13298

[23] Vanderbilt D 1990 *Phys. Rev.* B **41** 7892

[24] Monkhorst H J and Pack J D 1976 *Phys. Rev.* B **13** 5188

[25] Fischer T H and Almlof J 1992 *J. Phys. Chem.* **96** 9768

[26] Wentzcovitch R M, Martins J L and Price G D 1993 *Phys. Rev. Lett.* **70** 3947

[27] Karki B B, Stixrude L, Clark S J, Warren M C, Ackland G J and Crain J 1997 *Am. Mineral.* **82** 52

[28] Payne M C, Teter M P, Allan D C, Arias T A and Joannopolous J D 1992 *Rev. Mod. Phys.* **64** 1045

[29] Blanco M A, Francisco E and Luaña V 2004 *Comput. Phys. Commun.* **158** 57

[30] Blanco M A, Martín Pendás A, Francisco E, Recio J M and Franco R 1996 *J. Molec. Struct. Theochem* **368** 245

[31] Flórez M, Recio J M, Francisco E, Blanco M A and Martín Pendás A 2002 *Phys. Rev.* B **66** 144112

[32] Poirier J P 1991 *Introduction to the Physics of the Earth's Interior* (Oxford: Cambridge University Press)

[33] Francisco E, Recio J M, Blanco M A and Martín Pendás A 1998 *J. Phys. Chem.* **102** 1595

[34] Francisco E, Sanjurjo G and Blanco M A 2001 *Phys. Rev.* B **63** 094107

[35] Birch F 1978 *J. Geophys. Res.* **83** 1257

[36] Baltache H, Khenata R, Sahnoun M, Driz M, Abbar B and Bouhafs B 2004 *Phys.* B **344** 334

[37] Marinelli F and Lichanot A 2003 *Chem. Phys. Lett.* **367** 430

[38] Oganov A R and Dorogokupets P I 2003 *Phys. Rev.* B **67** 224110

[39] Oganov A R and Ono S 2004 *Nature* **430** 445

[40] Oganov A R and Brodholt J P 2000 *Phys. Chem. Miner.* **27** 430

[41] Hashin Z and Shtrikman S 1962 *J. Mech. Phys. Solids* **10** 343

[42] Karki B B and Wentzcovitch R M 2003 *Phys. Rev.* B **68** 224304